NeuroImage 197 (2019) 69–79

Contents lists available at ScienceDirect

NeuroImage

journal homepage: www.elsevier.com/locate/neuroimage

Dynamic origin of spike and wave discharges in the brain

Hossein Sohanian Haghighi, Amir H.D. Markazi *

School of Mechanical Engineering, Iran University of Science and Technology, Tehran, 16844, Iran

ARTICLE INFO

Keywords:
Spike-wave discharges
Absence epilepsy
Photosensitive epilepsy
Neural mass model
Stochastic resonance

ABSTRACT

Spike and wave discharges are the main electrographic characteristic of a number of epileptic brain disorders including childhood absence epilepsy and photosensitive epilepsy. The basic dynamic mechanism that underlies the occurrence of these abnormal electrical patterns in the brain is not well understood. The current paper aims to provide a dynamic explanation for features and generation mechanism of spike and wave discharges in the brain. The main proposition of this study is that epileptic seizures could be interpreted as a resonance phenomenon rather than a limit cycle behavior. To shows this, a revised version of Jansen-Rit neural mass model is employed. The system can switch between monostable and bistable regimes, which are considered in this paper as wake and sleep states of the brain, respectively. In particular, it is shown that, in monostable region, the model can depict the alpha rhythm and alpha rhythm suppression due to mental activity. Frequency responses of the model near the bistable regime demonstrate that high amplitude harmonic excitation may lead to spike and wave like oscillations. Based on the computational results and the concept of stochastic resonance, a model for absence epilepsy is presented which can simulate spontaneous transitions between ictal and interictal states. Finally, it is shown that spike and wave discharges during epileptic seizures can be explained as a resonance phenomenon in a nonlinear system.

1. Introduction

In 1935, a few short years after the discovery of the electroencephalogram (EEG) by Hans Berger, Gibbs and his colleagues presented a clear description of brain electrical activity during clinical seizures (Gibbs et al., 1935). They found large amplitude 3 Hz approximately sinusoidal waves including sharp negative spikes in EEGs from twelve patients with petit mal (absence) epilepsy. Since that time, spike-wave complexes are known as characteristic oscillatory patterns that can be observed in EEG signals during absence seizures. Absence seizures are often found in children typically between 4 and 10 years of age and cause lapses in consciousness (Stafstrom and Carmant, 2015). These seizures usually last 5–20 s and the frequency of occurrence varies from a few to hundreds per day. Seizures commonly start and end abruptly and the amplitude of complexes increases and the repetition frequency decreases during the ictal phase. SWDs are also associated with photosensitive epilepsy, a type of epilepsy induced by visual stimuli e.g. flashing or flickering lights (Fisher et al., 2005). Finding spike and wave pattern in EEG during intermittent photic stimulation is a common examination for the diagnosis of photosensitive epilepsy. Additionally, SWDs can be found in some other types of epilepsy such as Lennox-Gastaut syndrome and juvenile myoclonic epilepsy with a little difference in recurrence frequency of discharges (Stafstrom and Carmant, 2015).

Absence epilepsy is considered to be a brain disorder with a genetic aetiology (Crunelli and Leresche, 2002). There is a hot debate whether the location of SWD generators is in the cortex or the thalamus (Avoli, 2012). Experimental findings seem to be controversial (Blumenfeld, 2005) but more evidence support the cortical origin theory (Meeren et al., 2005, 2002) for human subjects (Moeller et al., 2010; Seneviratne et al., 2014). A fundamental question is whether the SWDs can be generated only in the cortex (or thalamus) or the interaction between cortical and sub-cortical areas is necessary.

Mathematical neural models are useful tools to study effects of various parameters and dynamic mechanisms underlying the brain state variations. Computational models of SWD could be divided into two main groups: thalamocortical models and network models (Wendling et al., 2016). Thalamocortical models consider the interactions of cortical and thalamic neuronal populations. Usually, both excitatory and inhibitory populations in cortex module and reticular nucleus and relay nuclei in thalamic module are modeled in a thalamocortical network. In order to develop such a thalamocortical model, Lopes da Silva and his group (Lopes da Silva et al., 2003) extended the alpha rhythm model (Lopes da

* Corresponding author.
E-mail address: markazi@iust.ac.ir (A.H.D. Markazi).

https://doi.org/10.1016/j.neuroimage.2019.04.047
Received 7 January 2019; Received in revised form 13 April 2019; Accepted 17 April 2019
Available online 23 April 2019

Silva et al., 1974) and then showed that the extended model has a bistable regime (coexistence of a fixed point and a limit cycle). So, the model was used to simulate spontaneous transitions between normal and epileptic states in a noisy environment (Suffczynski et al., 2004). In the same years, Robinson and his colleagues developed another cortico-thalamic model (Robinson et al., 2003, 2002). The model is sensitive to its parameters and depending to the parameters values, various dynamical regimes including 3 Hz spike and wave limit cycle can be found in the model (Breakspear et al., 2006; Deeba et al., 2018; Kim et al., 2009; Roberts and Robinson, 2008; Rodrigues et al., 2009; Yang and Robinson, 2017). Another group of researchers extended Amari neural field model (Amari, 1977) in order to develop another thalamocortical model (Taylor et al., 2013a) based on previous models of SWD (Taylor and Baier, 2011; Wang et al., 2012). It was shown that the model is excitable and so a seizure can be simulated as a transient response to stimulation. The model can also work in a bistable regime (Taylor et al., 2015) and in this case and in the absence of noise, if a second stimulus is not applied the SWD will never end. Besides these thalamocortical models, a number of network models are also available. Network models usually constructed by making networks of neuronal oscillators such as Hodgkin-Huxley model or Fitzhugh-Nagumo neural model in order to simulate SWDs in the brain (Destexhe, 2014, 2008; Medvedeva et al., 2018). However, studies of networks of neural mass models are also available in the literature (Goodfellow et al., 2012; Peter Neal Taylor et al., 2013a,b). Based on analysis of a network of coupled neural population models (Goodfellow et al., 2011) the authors introduced intermittency (spontaneous bursting behavior) as another possible dynamic mechanism of SWD.

The mentioned studies used various mathematical models and proposed different dynamic mechanisms such as bistability, bifurcation, excitability or intermittency (Baier et al., 2012) to describe transitions between ictal and interictal states. However, most of them have a common characteristic: at least one limit cycle attractor exists in the model. Noise, variation of parameters, perturbation or internal dynamics may push the dynamics into this limit cycle. Since more than one single mechanism may contribute to initiation and propagation of epileptic seizures in different cases, alternative descriptive mechanisms of transitions between normal and abnormal epileptic states should be taken into account. Moreover, there are a number of clinical and experimental observations that could not be explained straightforwardly when a limit cycle attractor is considered as the origin of SWDs. For example, initial studies by Steriade and colleagues showed that 3 Hz SWDs can be induced by 10 Hz electrical stimulation of the brain, in both the monkey (Steriade, 1974) and the cat (Steriade and Yossif, 1974). A recent study also revealed a causal relationship between rhythmic stimulation and seizure initiation in WAG/Rij rats using intracortical optogenetic stimulation (Wagner et al., 2015). The study also showed seizures were induced more effectively when the stimulation frequency is around 10 Hz. In addition, generalized 3 Hz spike and waves are the most common pattern in photoparoxysmal response to rhythmic visual stimulations (Fisher et al., 2005; Waltz et al., 1992). In general, there exists a lack of knowledge about the underlying dynamic mechanism responsible for such abnormal EEG response to visual stimulations at certain frequencies.

Here, and in line with our previous work (Sohanian Haghighi and Markazi, 2017), we hypothesis that epileptic seizures could be considered as a resonance phenomenon rather than a limit cycle behavior. To provide some computational evidence for this hypothesis, the well-known Jansen-Rit neural mass model is used. The model is first described and revised by a change in one of its parameters. Next, frequency responses of the revised model are obtained to find out possibility of spike and wave like response due to harmonic excitations. Finally, based on the obtained results, we try to explain some related clinical and experimental findings from a dynamical system point of view.

2. Jansen-Rit neural mass model

2.1. Model description

One of the earliest neural mass models which many other neural population models are developed based upon this model, is presented by Lopes da Silva (Lopes da Silva et al., 1974). The model contains of two kinds of neural populations, an excitatory population, representing pyramidal neurons and an inhibitory cell population, representing inhibitory interneurons. The two populations are connected via a feedback loop with two coupling constants that enables the model to simulate rhythmical activity of the brain. As it was also suggested in previous researches (Lopes da Silva et al., 1976; Zetterberg et al., 1978), Jansen add another excitatory population to the model that representing excitatory interneurons (Jansen et al., 1993; Jansen and Rit, 1995). Schematic of the model is presented in Fig. 1.a. Each population is modeled by an average membrane potential and an action potential firing rate, which are described mathematically by a dynamic linear transfer function and a static nonlinear operator. The linear transformations relate neural spiking activity to changes in membrane potential over time and the nonlinear element (e.g. sigmoidal) converts the membrane potential to the corresponding neuronal firing rate. A block diagram representation of the model is depicted in Fig. 1.b. The linear dynamic transformations are modeled by impulse responses $h_e(t)$ for the excitatory populations and $h_i(t)$ for the inhibitory population as below

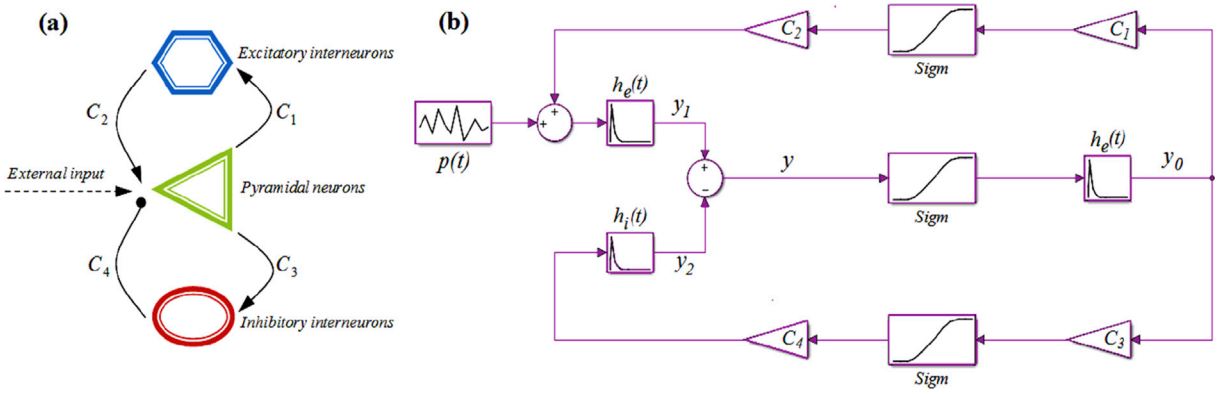

Fig. 1. (a) Interactions between a population of pyramidal neurons and populations of excitatory and inhibitory interneurons in Jansen-Rit neural mass model. Arrows indicate excitatory connections and circle end shows inhibitory connection. (b) Block diagram representation of the mathematical model. The h blocks simulate synapses in neuronal populations. The *Sigm* blocks transform membrane potential of each population into the corresponding neuronal firing rate. The constant gains C_i represent strengths of the synaptic connections between populations.

$$\begin{cases} h_e(t) = Ate^{-at}, t \geq 0 \\ h_i(t) = Bte^{-at}, t \geq 0 \end{cases} \quad (1)$$

where A and B are the excitatory and inhibitory average synaptic gains and a and b denote the membrane time constants. The nonlinear element converts the membrane potential to the corresponding neuronal firing rate by the following sigmoid shape function:

$$Sigm(v) = \frac{2e_0}{1 + e^{r(v_0 - v)}} \quad (2)$$

where, e_0, v_0 and r are the maximum firing rate, threshold and slope parameter, respectively. The constants C_1 to C_4 are the coupling terms and $y_0(t), y_1(t)$ and $y_2(t)$ represent the average membrane potentials of neural populations. The model is excited by an external input characterized by $p(t)$ (in pulses per second), representing the mean rate of incoming excitatory pulses from neighboring populations. The original model proposed in (Lopes da Silva et al., 1974) considered such a pulse rate to be a Gaussian white noise with a non-zero mean.

From the control theory point of view, Jansen-Rit neural mass model is composed of both positive and negative feedback loops in contrast to the original model, which has only a negative feedback loop. The model can be described mathematically by the following set of first order differential equations (Jansen and Rit, 1995):

Table 1
Physiological interpretation and standard values of the parameters in Jansen-Rit model.

Parameter	Description	Value
A	average excitatory synaptic gain	3.25 mV
B	average inhibitory synaptic gain	22 mV
a	average synaptic time constant for excitatory population	$100s^{-1}$
b	average synaptic time constant for inhibitory population	$50s^{-1}$
C	connectivity constant parameter	$C = 135$ (*standard value*) $C = 132$ (*current study*)
C_1, C_2	average number of synaptic contacts in the excitatory feedback loop	$C_1 = C,\ C_2 = 0.8C$
C_3, C_4	average number of synaptic contacts in the inhibitory feedback loop	$C_3 = 0.25C,\ C_4 = 0.25C$
e_0, v_0, r	parameters of sigmoid function	$v_0 = 6mV, e_0 = 2.5s^{-1}, r = 0.56mV^{-1}$

$$\begin{aligned} \dot{y}_0(t) &= y_3(t), \quad \dot{y}_3(t) = Aa\mathrm{Sigm}(y_1 - y_2) - 2ay_3(t) - a^2y_0(t) \\ \dot{y}_1(t) &= y_4(t), \quad \dot{y}_4(t) = Aa\{p(t) + C_2\mathrm{Sigm}[C_1y_0(t)]\} - 2ay_4(t) - a^2y_1(t) \\ \dot{y}_2(t) &= y_5(t), \quad \dot{y}_5(t) = BbC_4\mathrm{Sigm}[C_3y_0(t) - 2by_5(t) - b^2y_2(t) \end{aligned} \quad (3)$$

The model output $y = y_1 - y_2$, corresponds to the average membrane potential of the pyramidal cells, which is interpreted as an EEG signal. The standard values of the model parameters are listed in Table 1 (Jansen and Rit, 1995).

2.2. Bifurcation analysis

While Lopes da Silva model is developed to reproduce only the alpha rhythm activity of the brain, Jansen and Rit found that their extended model can simulate various brain rhythms when the value of the connectivity constant parameter, C, is changed. For example, they simulated the alpha rhythm with C = 135 and a uniformly distributed random input in the range 120–320 pulses per second (pps). There is a delicate but important difference between the dynamic mechanisms of alpha rhythm generation in Lopes da Silva model and in Jansen-Rit model. In the former, despite of the existence of a limit cycle regime in the nonlinear model (Zetterberg et al., 1978), the authors linearized the model and considered alpha rhythm response as a filtered noise. In the latter, based on a bifurcation analysis, it was revealed that alpha-like activity is due to the existence of a limit cycle attractor with a frequency about 10 Hz for the assumed range of input values (Grimbert and Faugeras, 2006). The mentioned study also showed that bifurcation analysis of Jansen-Rit model with respect to the input value and with non-nominal settings of the other parameters could lead to fairly different bifurcation diagrams. For example, it can be observed, as in Fig. 2, that by choosing a lower value (C = 132) instead of the nominal value (C = 135) for the connectivity constant parameter, limit cycle attractors completely disappear. Similar diagrams can be obtained, for a few percentages lower values of synaptic gains or higher values of average synaptic time constants. For the rest of this paper we considered C = 132 as a default value for the connectivity constant and set the other parameters to the nominal values as given in Table 1.

2.3. Potential-like function

By setting the derivatives in equation (3) to zero, the following system of equations is obtained:

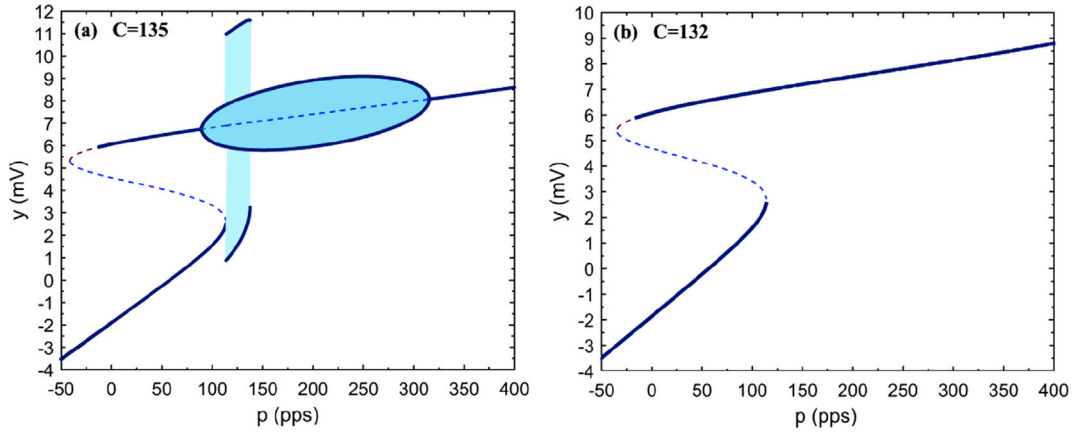

Fig. 2. Bifurcation diagrams of Jansen-Rit neural mass model with two different connectivity constants: (a) C = 135 and (b) C = 132. The diagrams show extrema of output values as a function of the constant input and are obtained by sweeping the input value in forward and backward direction and the initial conditions for the system integration are the final states in the previous step. Solid lines represent stable and dashed lines represent unstable states. Limit cycles correspond to shaded regions. In bistable regions, the model output depends on the initial conditions and so the directions of parameter changes are important in these regions. The negative input values have no physiological meaning and only serve for visual description of bifurcation diagrams.

$$\begin{cases} y_0 = \frac{A}{a} Sigm(y_1 - y_2), & y_3 = 0 \\ y_1 = \frac{A}{a}(p + C_2 Sigm(C_1 y_0)), & y_4 = 0 \\ y_2 = \frac{B}{b} C_4 Sigm(C_3 y_0), & y_5 = 0 \end{cases} \quad (4)$$

which leads to an implicit equation for equilibrium points ($y = y_1 - y_2$):

$$y = \frac{A}{a}p + \frac{A}{a}C_2 Sigm\left(\frac{A}{a}C_1 Sigm(y)\right) - \frac{B}{b}C_4 Sigm\left(\frac{A}{a}C_3 Sigm(y)\right) \quad (5)$$

This equation can be solved numerically to find equilibrium points for the assumed input value. Since there is no limit cycle in the bifurcation diagram for C = 132, the equilibrium curve as a function of the input value is identical to the bifurcation diagram shown in Fig. 2.b. Depending to the input value, the model may have either one or three equilibrium points. By analogy with mechanical equilibrium (at which the gradient of the potential energy is zero), a potential like function can be defined as below:

$$U(y) = \frac{1}{2}y^2 - \frac{A}{a}p\,y - \int_0^y \left[\frac{A}{a}C_2 Sigm\left(\frac{A}{a}C_1 Sigm(x)\right) - \frac{B}{b}C_4 Sigm\left(\frac{A}{a}C_3 Sigm(x)\right)\right] dx \quad (6)$$

So, at the equilibrium state, $\frac{\partial U}{\partial y}$ is zero. As shown in Fig. 3, the shape of this function depends on the input value. For positive input values lower than $p = 114\ pps$, three equilibrium states exist while for larger input values, the system has just a single equilibrium point. Furthermore, bistability occurs for low mean rate of excitatory input pulses and a dc potential shift is associated with changing the equilibrium point in the bistable region. It is reported in the literature that lower firing rates and dc shifts are observed during sleep state of the brain (Marshall et al., 1998; Vyazovskiy et al., 2009). Hence, one may interpret the monostable and bistable regimes of Fig. 2.b as wake and sleep states of the brain, respectively.

3. Results

In order to explore the model dynamics in monostable region of Fig. 2b, a sinusoidal waveform signal is added to input of the model, which was originally a biased white noise:

$$p(t) = p_0 + p_n + p_s \sin(2\pi f_s t) \quad (7)$$

Here, p_0 is bias, p_n is Gaussian white noise with zero mean and standard deviation, σ_n and p_s and f_s are amplitude and frequency of the sinusoidal component. The Gaussian noise is generated with 40 Hz constant sampling frequency. Frequency responses of the model are obtained in the absence of the noise and response amplitudes are defined as half of the steady-state peak-to-peak amplitude of the time response. The model equations (eq. (3)) are solved numerically by using the same method (Runge-Kutta-Fehlberg method) as the original paper (Jansen and Rit, 1995) with a sufficiently small relative tolerance ($<10^{-10}$). The initial conditions are the static equilibrium state for each simulated case.

3.1. Resonance in monostable region

For the time invariant input values higher than $p = 315\ pps$, Jansen-Rit model with nominal parameters has only one equilibrium point. By changing the connectivity parameter into C = 132, regions with limit cycle dynamics disappear and the monostable region appears in a wider range of input values. In the absence of noise and for small amplitude of excitation ($p_s = 5\ pps$), the model works like an underdamped second order system. Interestingly, for a wide range of mean input values, the resonance frequency remains near the alpha peak frequency and the equivalent damping ratio increases as the dc component increases. So, as it can be seen in Fig. 4, the peak amplitude in the frequency response curve suppresses as the mean value of the input is raised. The amplitude suppression in alpha band frequency mimics the alpha rhythm attenuation in the EEG signals caused by opening the eyes or by intense mental activity. This will be discussed further in Section 4.1. From Fig. 4, it can be seen that, in monostable region, the Jansen-Rit model works like a band pass filter for noisy input. Hence, alpha rhythm and alpha suppression phenomena can be explained by this model. In order to study the effect of increasing the bias value on the attenuation of the oscillation amplitude, the response due to a biased white noise input is presented in Fig. 5, revealing that a fast decaying high amplitude output appears after the mean input value increases suddenly (see Fig. 5b).

3.2. Frequency response near the bistable regime

In this section, the frequency response of the model is evaluated when the system operates near the bistable regime. The model shows bistability for positive constant input values below $p \approx 114\ pps$. Here, we assumed $p_0 = 125\ pps$ which is close enough to the bistable region for our study. Frequency responses of the system subjected to biased sinusoidal inputs are obtained in the absence of noise. In order to illustrate the effects of driving amplitude, three different levels of excitation are considered. Fig. 6.a shows for small level of excitation ($p_s = 5\ pps$), the system oscillates within monostable region and behaves like an underdamped second order linear oscillator. When p_s increases to $15\ pps$, bending in the frequency response curve is observed and the resonance frequency shifts to lower values. In this case, the system behaves as a softening nonlinear oscillator. Since the potential-like function (see eq. (6)) is actually time-variant when the input has a dynamic component, the system may switch between monostable and bistable regions of Fig. 2.b for strong excitations. Therefore, when the level of excitation is sufficiently large, e.g. $p_s = 30\ pps$, the system can oscillate between the two potential wells (inter-well dynamics). In this situation, there are three possible stable steady-state responses: a small amplitude intra-well

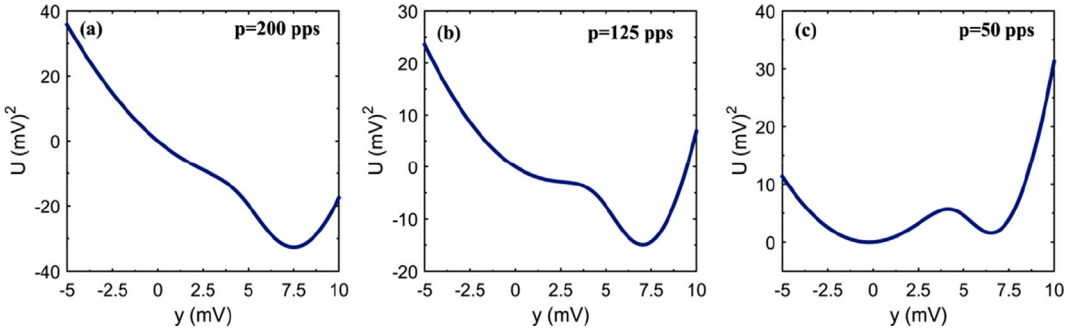

Fig. 3. The potential-like function for three different input values: (a) $p = 200\ pps$, (b) $p = 125\ pps$ and (c) $p = 50\ pps$. Decrease in input value leads to emerging an additional stable fixed point and an unstable equilibrium.

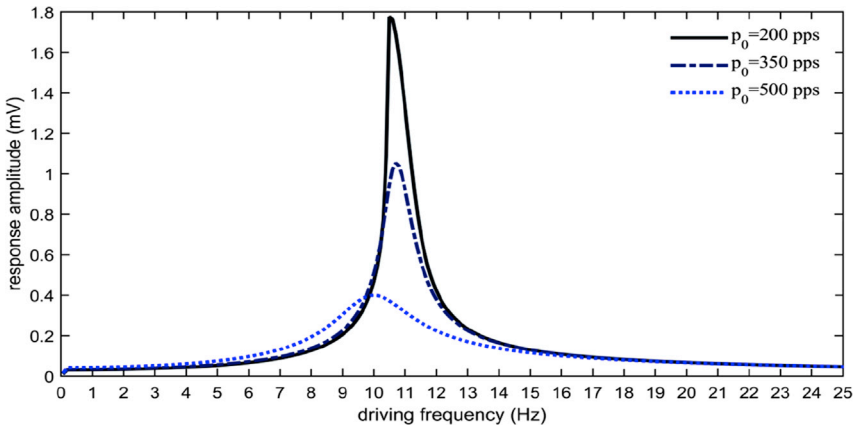

Fig. 4. The influence of the mean input firing rate p_0, on frequency response of the model subjected to biased harmonic excitation with a constant amplitude, $p_s = 5\,pps$.

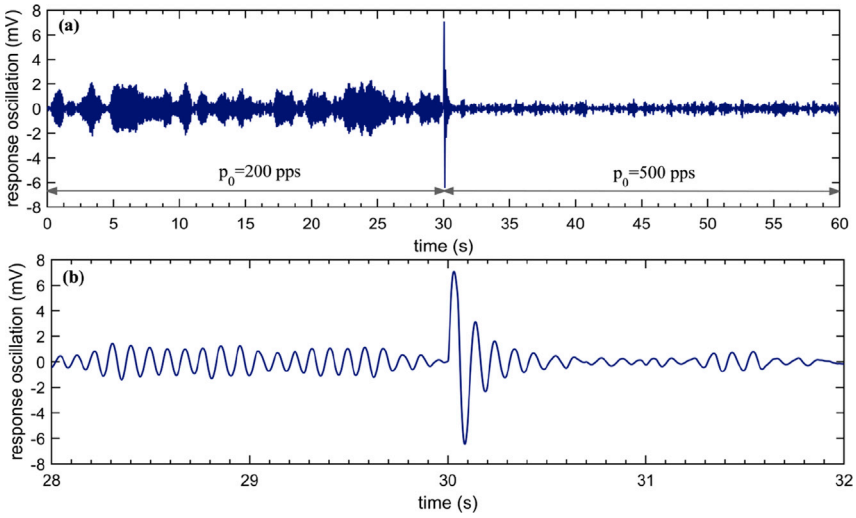

Fig. 5. Output of the model subjected to biased white noise ($p_s = 0$) with $\sigma_n = \sqrt{20}$ pps . (a) Alpha rhythm and alpha rhythm suppression because of a sudden increase in the mean input firing rate at second 30 from $p_0 = 200$ pps to $p_0 = 500$ pps. (b) Details of the transient response after the change in mean input value.

oscillation, a medium amplitude intra-well oscillation, and a large amplitude inter-well oscillation. During inter-well oscillation, the response waveform is a complex of a fast spike in one well and a slow wave in the other well. The frequency of repetition of this spike and wave complex is considerably lower than the excitation frequency because oscillations is slower in one well compared to the other well. As a result of the inter-well oscillatory region, a discontinuity is observed in the resonance branch. The model also produces superharmonic resonance at about one-half of the fundamental frequency for high excitation levels. Since the system is nonlinear, as it can found in Fig. 6.d-f, the model responses are not completely sinusoidal especially when the response amplitude increases near the resonance frequency. The fundamental and second harmonics are clearly visible by the darker shading spectral. As the level of excitation increases, higher harmonic components become more visible because the response waveform deviates more from the sinusoidal shape. Fig. 6.f reveals a dramatic increase in power at about 3 Hz and its harmonics when the driving frequency is in the range [8.6, 9.1], which describes spike and wave like dynamics in the model.

Fig. 7 illustrates transitions from static to steady state large amplitude oscillatory dynamics for each excitation level. The repetition frequency is close to the excitation frequency for $p_s = 5\,pps$ and $p_s = 15\,pps$ as it can be seen in Fig. 7a, b. However, for the case $p_s = 30\,pps$, the response main frequency is about one-third of the excitation frequency. This 3 Hz spike-wave like response is shown in Fig. 7.c.

3.3. A model for spike-wave seizures

In the previous section, frequency responses of the model obtained in the absence of noise. However, the brain is a complex network of billions of neurons that respond to various internal and external perturbations. EEG findings also confirm that a real input to a cortical population is not a pure sinusoidal wave with constant amplitude and frequency. Brain signals also are not just white noise and usually are described by rhythmic activities in specific frequency bands. So, in order to have a more realistic model for the input, both harmonic and noisy components are considered in this section. The harmonic component can be regarded as rhythmic activity in the brain (e.g. alpha rhythm) and the noisy component represents background activity that does not contain a dominant characteristic frequency. Combination of noise and a periodic excitation in a bistable system may lead to stochastic resonance, a dynamic mechanism by which irregular fluctuations amplify the response of the system to weak periodic input (Wiesenfeld and Moss, 1995). Here, we are interested to the case that the noise is not strong enough to cause a steady state stochastic resonance but its intensity is sufficient to produce a transient high amplitude oscillation. Results of simulation of the model with $p_s = 20$ pps, $f_s = 8.5\,Hz$ and $\sigma_n = \sqrt{24}$ pps are presented in Fig. 8. The amplitude and frequency of the harmonic component are chosen such that the model produces a small amplitude intra-well oscillation in the absence of noise. Fig. 8.a shows the model can generate both normal

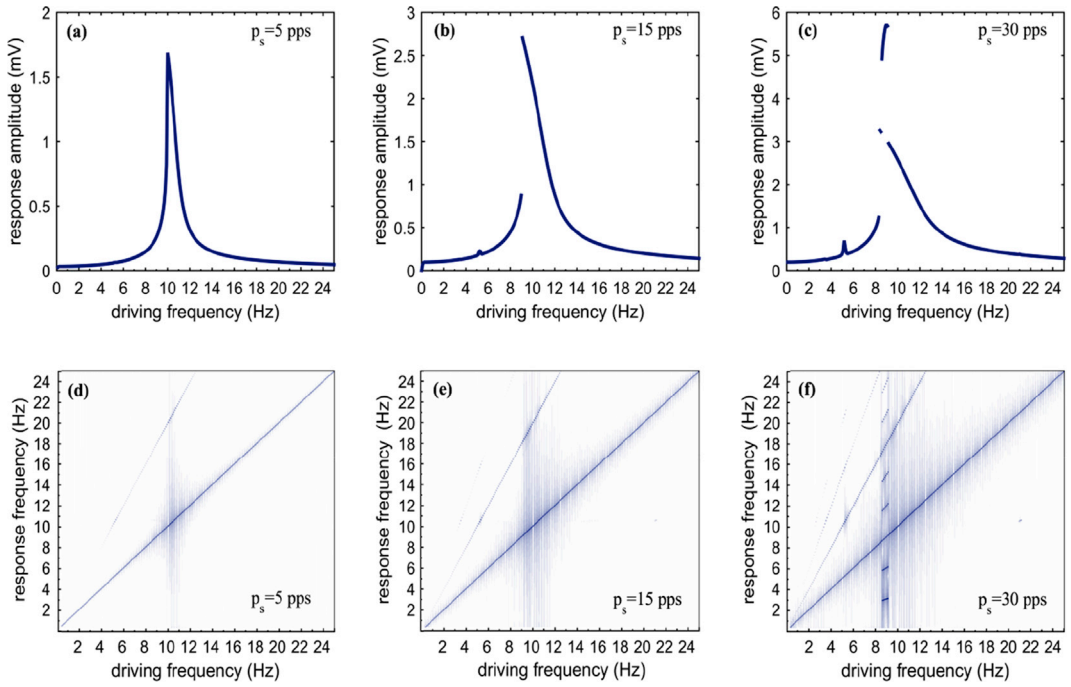

Fig. 6. Frequency response curves and corresponding spectral responses for three different excitation amplitudes with $p_0 = 125$ pps. Diagrams (a), (b) and (c) are frequency response curves for $p_s = 5$ pps, $p_s = 15$ pps and $p_s = 30$ pps, respectively. Diagrams (d), (e) and (f) are spectral responses for $p_s = 5$ pps, $p_s = 15$ pps and $p_s = 30$ pps, respectively and darker shading in these diagrams indicates higher power.

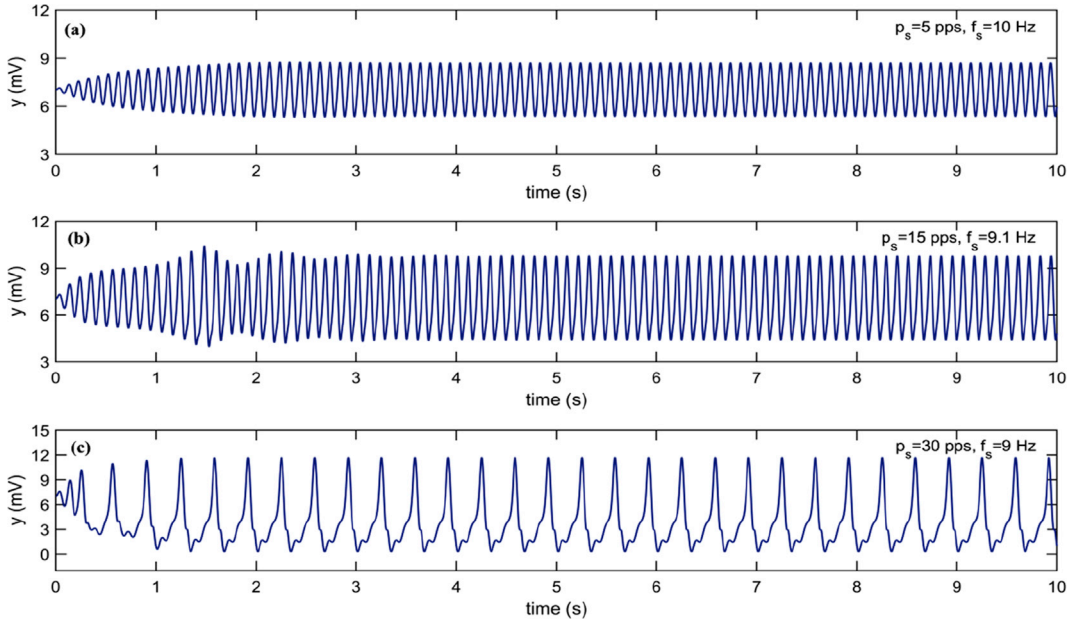

Fig. 7. Time histories of resonant responses with $p_0 = 125$ pps and for three excitation levels: (a) $p_s = 5$ pps, (b) $p_s = 15$ pps and (c) $p_s = 30$ pps.

activity and spike-wave discharges. Transitions between these two states occur spontaneously and without any changes in the model parameters. The model simulates two seizures during 400 s of simulation time, which are shown in detail in Fig. 8b, c. Three-hertz high amplitude spike and wave pattern is observed in diagram of the first simulated seizure (see Fig. 8b). The pattern also contains double spikes. As soon as the 3 Hz spike and wave discharges terminate, the normal activity immediately returns to the simulated signal. The second simulated seizure is more complex. As it is shown in Fig. 8c, a mix of medium amplitude intra-well oscillation and high amplitude inter-well oscillation is seen in this diagram. The model can produce seizure like outputs and simulated seizures are not identical due to nonlinearity and stochastic component of the model.

4. Discussion

The current study was based on the hypothesis that the brain works like a resonator, which can be excited by either internal or external sources. This hypothesis is supported by findings of brain stimulation experiments with different techniques including sensory stimulation (Herrmann, 2001; Spiegler et al., 2011; Zaehle et al., 2010), transcranial magnetic stimulation (Rosanova et al., 2009) and transcranial alternating

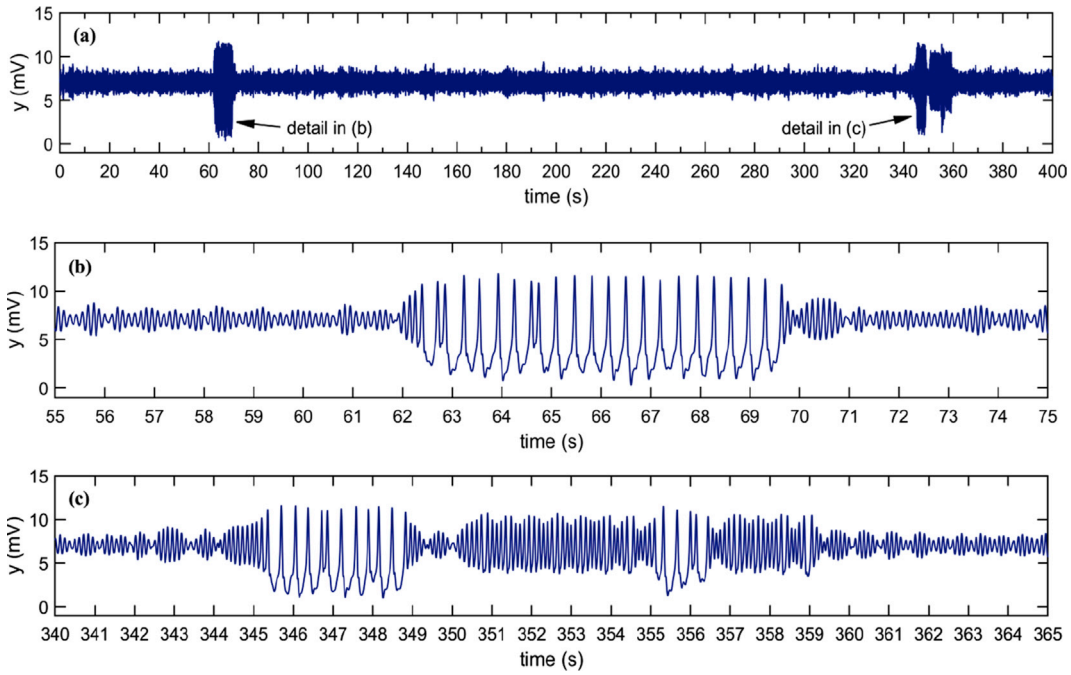

Fig. 8. Results of simulation of the model subjected to combination of non-zero mean harmonic excitation and white noise. The input is provided by $p(t) = p_0 + p_s \sin(2\pi f_s t) + p_n$ with $p_0 = 125$ pps, $p_s = 20$ pps and $f_s = 8.5$ *Hz*. Also p_n is Gaussian white noise with zero mean and standard deviation $\sigma_n = \sqrt{24}$ pps. Model output during 400 s simulation of the model is shown in diagram (a). Details of large amplitude oscillation regimes are presented in diagrams (b) and (c).

current stimulation (Helfrich et al., 2014). The brain response to a periodic stimulus (e.g. a flashing light) may also reveal some nonlinear characteristics such as subharmonic resonances in the brain response (Lazarev et al., 2001; Salchow et al., 2016; Schwab et al., 2006). Such nonlinear behaviors also reported in computational neural models (Herrmann et al., 2016; Labecki et al., 2016; Roberts and Robinson, 2012; Sohanian Haghighi and Markazi, 2017; Veltz and Sejnowski, 2015). In the current study, Jansen-Rit neural mass model subjected to periodic excitation is investigated. The model is interesting to researchers mainly because of its rich dynamics, which include two limit cycles. While the monostable region with a stable fixed point (see Fig. 2a) is usually neglected, we extended this region by shifting the connectivity parameter to a slightly lower value (see Fig. 2b). Results of the frequency response of the model in the monostable region reveal several interesting characteristics, which will be discussed in the following.

4.1. Alpha rhythm and alpha blocking

Alpha waves are sinusoidal-like oscillations appear in the electroencephalogram within the frequency range of 8–13 Hz and can be recorded best from the posterior head regions in a wakefulness and relaxed state with eyes closed and relatively mental inactivity. Since Berger's discovery of this rhythm in human EEG, understanding the generation mechanism has been a topic of research. From a dynamical system point of view, the rhythm may be a form of filtered noise (Lopes da Silva et al., 1974) or an oscillatory behavior due to a stable limit cycle (Burke and de Paor, 2004). Most of experimental data analysis support the idea of generation of this rhythm by band-pass filtering of noisy inputs in cortical networks (Hindriks et al., 2011; Lopes da Silva et al., 1997; Nunez, 2000; Stam et al., 1999). When a linear filter is considered, this view is challenged by observation of nonlinear behavior in the brain response to a periodic stimulation (Gebber et al., 1999; Miranda de Sá and Infantosi, 2005). However, the original model of brain alpha rhythm (Lopes da Silva et al., 1974) contained nonlinear elements and so the filter may work like a nonlinear resonator and nonlinear responses of the brain can be explained by considering the nonlinear nature of the filter (Labecki et al., 2016). As it was mentioned earlier, the alpha rhythm in Jansen-Rit model is usually known to be as a result of a limit cycle attractor. However, the model also has a monostable regime (with a stable fixed point) within which the model has a resonant frequency close to the alpha band peak frequency. Hence, we can return to the original modeling philosophy (Lopes da Silva et al., 1974) by focusing on this monostable fixed point regime. As it was shown in Fig. 2, the monostable region can be extended by changing the model parameters, (e.g. the connectivity constant parameter) and removing limit cycles from the bifurcation diagram. The model can also generate nonlinear responses and superharmonic resonance as it was shown in Fig. 6. In addition, because of bending in the frequency response curve, higher alpha amplitudes lead to slower alpha frequencies. These results are consistent with clinical EEG findings (Ernst Niedermeyer and Lopes da Silva, 2005).

Berger's initial examinations also revealed that alpha rhythm amplitudes become suppressed after eyes opening (Berger effect). The rhythm was also attenuated or blocked by attention and mental activity. There are a few computational models for such behavior in the literature (Suffczynski et al., 2001). In this paper, it was shown that the monostable regime in Jansen-Rit model has an interesting characteristic. The resonance frequency of the model remains nearly constant for a wide range of incoming mean firing rates while the amplitude of oscillation decreases as the input increases within this range. In contrast to (Hindriks and van Putten, 2013), this change in the amplitude of model response is caused by changing the input mean value and not the model parameters. The relation between the mean spiking rate and alpha activity is demonstrated in an animal study (Haegens et al., 2011). This study showed spiking rate is negatively associated with alpha power, i.e. as the firing rate increases alpha power decreases. In another recent study, the spiking rate increases during attention (Ruff and Cohen, 2016). Therefore, the reverse relation between the incoming firing rate and alpha rhythm power as shown in Fig. 4 is in agreement with the available experimental findings.

4.2. Spike-wave discharges, lapse of consciousness and absence epilepsy

According to Fig. 2.b, the presented model has two distinct regions for positive constant input values: a monostable region for mean firing rates

above 114 pps, which represent the wake state, and a bistable region for lower input values, which can be considered as sleep state. In the current study however, we focused on the monostable region of Fig. 2.b and analysis of the model behavior in the bistable region remains for future works. We have shown through frequency response analysis of the model that SWD can be found in the model response when the system works near the bistable region (sleep state). In this condition, the mean firing rate is near the lower bound of the monostable region (wake state). This result is in line with the clinical observations since absence seizures are mainly characterized by impairment of consciousness and predominantly occur during drowsiness (Sadleir et al., 2008), light NREM sleep (Halász, 2015) or arousals from sleep (Malow et al., 2000). Another activator of absence seizures is hyperventilation (Salvati and Beenhakker, 2019). Voluntary hyperventilation, with the resulting hypocapnia, reduces cerebral blood flow and causes slowing of the brain activity just as sleep and drowsiness (Patel and Maulsby, 1987). So, it can be considered as a technique to bring the brain state near the bistable regime and facilitate inter-well oscillations.

From dynamical point of view, when the system is near the bistable region (for stationary inputs) a strong excitation may lead to a transition to the bistable region. Hence, inter-well oscillations may be observed when the system is subjected to a strong harmonic driving. Based on results of the current study, 3 Hz spike and wave discharges can be interpreted as inter-well oscillations in a nonlinear system with asymmetric double well potential. Because of asymmetric shape of the potential well, the frequency of oscillation differs when the region of oscillation changes and slower dynamic response is observed in one well relative to the other well. Therefore, an inter-well oscillation composed of a fast dynamics and a slow dynamics as can be observed in spike and wave discharges pattern. The proposed dynamic description is illustrated in Fig. 9 schematically using a simple mechanical model of a ball moving between troughs.

Changing intra-well oscillation into inter-well oscillation requires relatively high excitation amplitude. One may consider alpha rhythm of the brain as the internal source of the harmonic input in the proposed scenario. Interestingly, alpha rhythm power usually is greater in the second half of the first decade of life (Petersén and Eeg-Olofsson, 1971) and children absence seizures typically occur in this period. In addition, there are evidence for a greater alpha rhythm power in children with epilepsy (Michels et al., 2011). High amplitude excitation also may come from an external source and based on the results of the current study, SWDs can be induced effectively when the stimulation frequency is close to the resonance frequency of the brain. This hypothesis is supported by experimental results in animal models (Steriade, 1974; Steriade and Yossif, 1974).

The genetic rodent models of absence seizures such as GAERS and WAG/Rij are widely used for studying the spike and wave discharges. While there are similarities between spike and wave discharges in these animal models and absence seizures in humans, the frequency of discharges in rodent models is generally higher; e.g., SWDs occur in rat with a fundamental frequency of 8–10 Hz (Coenen and Van Luijtelaar, 2003). Currently, the reasons for such difference is not fully understood, however, according to a computational study, a difference in the balance between slow and fast inhibitory receptors may cause a higher frequency of discharges in rodents (Destexhe, 1999). This hypothesis is based on a modeling approach at the neuronal scale and is a cellular scenario. At the macroscopic scale, however, the fast version of SWDs can be also explained as a resonance phenomenon. Because of bending in the frequency response curve (see Fig. 6 b), jumps between low amplitude and large amplitude branches is possible to occur, resembling abrupt transitions between ictal and interictal states. In addition, bending in the frequency response also leads to a decrease in the resonance frequency (see Fig. 6a, b). As observed in Fig. 6.e, because of asymmetric shape of the potential well, higher harmonics appear in the high amplitude response, which resembles fast SWDs in rodent models. In this case, fast and slow dynamics are due to large amplitude intra-well oscillation in an asymmetric potential well instead of the inter-well transitions. More details of this scenario can be found in our previous work (Sohanian Haghighi and Markazi, 2017). Based on this description, the fast version of SWD also may occur because of a resonance in the brain network. One can test this hypothesis by harmonic stimulation of the brain in rat models. Currently, there are some animal studies that support this scenario (Uhlrich et al., 2005; Wagner et al., 2015). Also, an increase in alpha power is predicted before transition from interictal to ictal activities as revealed in some experimental studies (Polack et al., 2007).

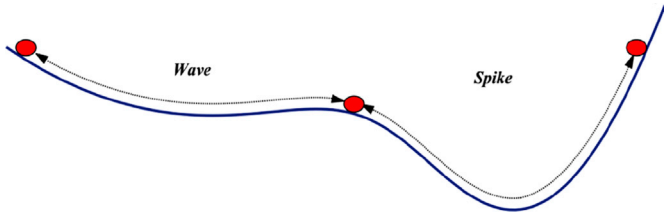

Fig. 9. Schematic illustration of spike and wave discharges. An asymmetric double well potential can lead to a complex of slow and fast dynamic response similar to motion of a ball rolling on an asymmetric surface under the influence of gravity.

Most of previous computational models of absence epilepsy are in the category of thalamocortical models. Usually, transitions between ictal and interictal states are described mathematically as transitions between a normal steady state and a limit cycle attractor due to a change in model parameters (Breakspear et al., 2006; Roberts and Robinson, 2008; Rodrigues et al., 2009). Various dynamical behaviors including polyspike-wave and spike-wave are simulated through this modeling approach (Marten et al., 2009a). Another common scenario is based on coexisting attractor dynamics. In this case, state transitions are caused by noisy inputs or random fluctuation of parameters in a bistable regime (Fröhlich et al., 2010; Marten et al., 2009b; Suffczynski et al., 2004). However, up to now, there is no clear and direct empirical evidence to support either of these scenarios. Moreover, a common drawback of available thalamocortical models as well as coupled neural mass models (Ahmadizadeh et al., 2018; Peter Neal Taylor et al., 2013) is their large number of parameters. Complexities of most of these models make it hard to understand the underlying physiological mechanisms. Hence, finding a relationship between theoretical findings and experimental results is in fact a challenging task. The general concept of the proposed model in the current study is different from pre-existing ones. The main idea for state transitions in the presented model is based on the concept of stochastic resonance which was previously shown to be a possible mechanism for interpreting brain dynamics (Aihara et al., 2010; Balázsi and Kish, 2000; Mori and Kai, 2002a, 2002b). We used the well-known Jansen-Rit neural mass model, which has relatively small number of parameters, while the dynamics depicted by the revised version of the model is not too complex. In addition, as discussed above, some clinical and experimental observations could be explained by this model. The simplicity of the model, however, could lead to some limitations. For example, spatio-temporal dynamics are neglected and complex waveforms such as polyspike-wave could not be reproduced by this model.

Returning to the question of the necessity of thalamocortical interaction in generation SWD, it should be noted the neural mass model used in this study considered the interactions of one inhibitory and two excitatory neural populations. Such interactions can be found in both cortex and thalamus. Recently, evidence for cortical origin of SWDs motivates researchers to develop computational models for seizures in an isolated cortex (Zhao and Robinson, 2017). The current study also supported cortical origin theory (Meeren et al., 2005, 2002) from a dynamical point of view and showed it would be possible that SWDs initiate in a cortical area due to interactions between excitatory and inhibitory neural populations in that area. However, our modeling approach does not reject the role of thalamus and it may act as a bridge between cortical areas in propagation of seizures.

4.3. Spike and wave discharges in photosensitive epilepsy

Epileptic seizure in photosensitive epilepsy patients is most frequently is elicited by a flash frequency about 10 Hz when the eyes are closed (Nagarajan et al., 2003) and 15–18 Hz flicker stimulus when the eyes are open (Lopes da Silva and Harding, 2011; Topalkara et al., 1998). While Fig. 6c, f clearly reveals spike and wave discharges for periodic excitation with a frequency near the alpha peak frequency, explanation for photoparoxysmal response due to 15–18 Hz stimulus is a little more complex. Both experimental and computational studies provide evidence of subharmonic resonance in this range of frequencies (Herrmann, 2001; Herrmann et al., 2016; Labecki et al., 2016; Roberts and Robinson, 2012). High amplitude oscillation due to subharmonic resonance with a frequency about half of the flash frequency may be converted to inter-well spike and wave oscillation. For example, photic stimulation with a frequency about 18 Hz may lead to large amplitude response with a frequency about 9 Hz in one area of the brain (for example in thalamus). According to the results of the current study, these large amplitude oscillations could cause 3 Hz spike and wave discharges in a relating region (for example in visual cortex). So, photoparoxysmal response to 15–18 Hz stimulus dynamically can be described as a subharmonic resonance in a nonlinear system with an asymmetric double well potential.

5. Conclusion

In this study, we tried to explain underling dynamic mechanism of spike and wave discharges in the brain. The well-known Jansen-Rit neural mass model was first refreshed by revising the connectivity constant parameter. Bifurcation analysis showed the revised model has two distinct regions for constant inputs: a monostable region with a fixed point (wake state) and a bistable region with two stable fixed points (sleep state). Frequency response of the model in the monostable regime subjected to low amplitude sinusoidal input reveals the model can be used to simulate both the alpha rhythm and alpha rhythm suppression in the wake state of the brain. Near the bistable regime, frequency response analysis revealed that high amplitude harmonic excitation may lead to inter-well oscillations, which resemble spike and wave oscillatory patterns. In addition, we demonstrated the system is excitable near the bistable regime and a transition to ictal state can be modeled through stochastic resonance concept. Finally, we highlighted the importance of our results and their relevance to clinical and experimental findings. We concluded that both absence seizures and photoparoxysmal response could be described as resonance phenomena in the brain.

References

Ahmadizadeh, S., Karoly, P.J., Nešić, D., Grayden, D.B., Cook, M.J., Soudry, D., Freestone, D.R., 2018. Bifurcation analysis of two coupled Jansen-Rit neural mass models. PLoS One 13, e0192842. https://doi.org/10.1371/journal.pone.0192842.

Aihara, T., Kitajo, K., Nozaki, D., Yamamoto, Y., 2010. How does stochastic resonance work within the human brain? - psychophysics of internal and external noise. Chem. Phys. 375, 616–624. https://doi.org/10.1016/j.chemphys.2010.04.027.

Amari, S., 1977. Dynamics of pattern formation in lateral-inhibition type neural fields. Biol. Cybern. 27, 77–87. https://doi.org/10.1007/BF00337259.

Avoli, M., 2012. A brief history on the oscillating roles of thalamus and cortex in absence seizures. Epilepsia 53, 779–789. https://doi.org/10.1111/j.1528-1167.2012.03421.x.

Baier, G., Goodfellow, M., Taylor, P.N., Wang, Y., Garry, D.J., 2012. The importance of modeling epileptic seizure dynamics as spatio-temporal patterns. Front. Physiol. 3 (JUL), 1–7. https://doi.org/10.3389/fphys.2012.00281.

Balázsi, G., Kish, L.B., 2000. From stochastic resonance to brain waves. Phys. Lett. 265, 304–316. https://doi.org/10.1016/S0375-9601(99)00894-4.

Blumenfeld, H., 2005. Cellular and network mechanisms of spike-wave seizures. Epilepsia 46 (Suppl. 9), 21–33. https://doi.org/10.1111/j.1528-1167.2005.00311.x.

Breakspear, M., Roberts, J.A., Terry, J.R., Rodrigues, S., Mahant, N., Robinson, P.A., 2006. A unifying explanation of primary generalized seizures through nonlinear brain modeling and bifurcation analysis. Cerebr. Cortex 16, 1296–1313. https://doi.org/10.1093/cercor/bhj072.

Burke, D.P., de Paor, A.M., 2004. A stochastic limit cycle oscillator model of the EEG. Biol. Cybern. 91, 221–230. https://doi.org/10.1007/s00422-004-0509-z.

Coenen, A.M.L., Van Luijtelaar, E.L.J.M., 2003. Genetic animal models for absence epilepsy: a review of the WAG/Rij strain of rats. Behav. Genet. 33, 635–655. https://doi.org/10.1023/A:1026179013847.

Crunelli, V., Leresche, N., 2002. Childhood absence epilepsy: genes, channels, neurons and networks. Nat. Rev. Neurosci. 3, 371–382. https://doi.org/10.1038/nrn811.

Deeba, F., Sanz-Leon, P., Robinson, P.A., 2018. Dependence of absence seizure dynamics on physiological parameter evolution. J. Theor. Biol. 454, 11–21. https://doi.org/10.1016/j.jtbi.2018.05.029.

Destexhe, A., 1999. Can GABA A conductances explain the fast oscillation frequency of absence seizures in rodents? Eur. J. Neurosci. 11, 2175–2181. https://doi.org/10.1046/j.1460-9568.1999.00660.x.

Destexhe, A., 2008. Corticothalamic feedback. In: Computational Neuroscience in Epilepsy. Elsevier, pp. 184–214. https://doi.org/10.1016/B978-012373649-9.50016-8.

Destexhe, A., 2014. Network models of absence seizures. In: Neuronal Networks in Brain Function, CNS Disorders, and Therapeutics. Elsevier, pp. 11–35. https://doi.org/10.1016/B978-0-12-415804-7.00002-2.

Fisher, R.S., Harding, G., Erba, G., Barkley, G.L., Wilkins, A., Epilepsy Foundation of America Working Group, 2005. Photic- and pattern-induced seizures: a review for the epilepsy foundation of America working group. Epilepsia 46, 1426–1441. https://doi.org/10.1111/j.1528-1167.2005.31405.x.

Fröhlich, F., Sejnowski, T.J., Bazhenov, M., 2010. Network bistability mediates spontaneous transitions between normal and pathological brain states. J. Neurosci. 30, 10734–10743. https://doi.org/10.1523/JNEUROSCI.1239-10.2010.

Gebber, G.L., Zhong, S., Lewis, C., Barman, S.M., 1999. Human brain alpha rhythm: nonlinear oscillation or filtered noise? Brain Res. 818, 556–560. https://doi.org/10.1016/S0006-8993(98)01303-1.

Gibbs, F.A., Davis, H., Lennox, W., 1935. The electro-encephalogram in epilepsy and in conditions of impaired consciousness. Arch. Neurol. Psychiatr. 34, 1133. https://doi.org/10.1001/archneurpsyc.1935.02250240002001.

Goodfellow, M., Schindler, K., Baier, G., 2011. Intermittent spike-wave dynamics in a heterogeneous, spatially extended neural mass model. Neuroimage 55, 920–932. https://doi.org/10.1016/j.neuroimage.2010.12.074.

Goodfellow, M., Schindler, K., Baier, G., 2012. Self-organised transients in a neural mass model of epileptogenic tissue dynamics. Neuroimage 59, 2644–2660. https://doi.org/10.1016/j.neuroimage.2011.08.060.

Grimbert, F., Faugeras, O., 2006. Bifurcation analysis of Jansen's neural mass model. Neural Comput. 18, 3052–3068. https://doi.org/10.1162/neco.2006.18.12.3052.

Haegens, S., Nacher, V., Luna, R., Romo, R., Jensen, O., 2011. α-Oscillations in the monkey sensorimotor network influence discrimination performance by rhythmical inhibition of neuronal spiking. Proc. Natl. Acad. Sci. Unit. States Am. 108, 19377–19382. https://doi.org/10.1073/pnas.1117190108.

Halász, P., 2015. Are absence epilepsy and nocturnal frontal lobe epilepsy system epilepsies of the sleep/wake system? Behav. Neurol. 2015, 231676. https://doi.org/10.1155/2015/231676.

Helfrich, R.F., Schneider, T.R., Rach, S., Trautmann-Lengsfeld, S.A., Engel, A.K., Herrmann, C.S., 2014. Entrainment of brain oscillations by transcranial alternating current stimulation. Curr. Biol. 24, 333–339. https://doi.org/10.1016/j.cub.2013.12.041.

Herrmann, C.S., 2001. Human EEG responses to 1-100 Hz flicker: resonance phenomena in visual cortex and their potential correlation to cognitive phenomena. Exp. Brain Res. 137, 346–353. https://doi.org/10.1007/s002210100682.

Herrmann, C.S., Murray, M.M., Ionta, S., Hutt, A., Lefebvre, J., 2016. Shaping intrinsic neural oscillations with periodic stimulation. J. Neurosci. 36, 5328–5337. https://doi.org/10.1523/JNEUROSCI.0236-16.2016.

Hindriks, R., van Putten, M.J.A.M., 2013. Thalamo-cortical mechanisms underlying changes in amplitude and frequency of human alpha oscillations. Neuroimage 70, 150–163. https://doi.org/10.1016/j.neuroimage.2012.12.018.

Hindriks, R., Bijma, F., van Dijk, B.W., van der Werf, Y.D., van Someren, E.J.W., van der Vaart, A.W., 2011. Dynamics underlying spontaneous human alpha oscillations: a data-driven approach. Neuroimage 57, 440–451. https://doi.org/10.1016/j.neuroimage.2011.04.043.

Jansen, B.H., Rit, V.G., 1995. Electroencephalogram and visual evoked potential generation in a mathematical model of coupled cortical columns. Biol. Cybern. 73, 357–366.

Jansen, B.H., Zouridakis, G., Brandt, M.E., 1993. A neurophysiologically-based mathematical model of flash visual evoked potentials. Biol. Cybern. 68, 275–283. https://doi.org/10.1007/BF00224863.

Kim, J.W., Roberts, J.A., Robinson, P.A., 2009. Dynamics of epileptic seizures: evolution, spreading, and suppression. J. Theor. Biol. 257, 527–532. https://doi.org/10.1016/j.jtbi.2008.12.009.

Labecki, M., Kus, R., Brzozowska, A., Stacewicz, T., Bhattacharya, B.S., Suffczynski, P., 2016. Nonlinear origin of ssvep spectra: a combined experimental and modeling study. Front. Comput. Neurosci. 10, 129. https://doi.org/10.3389/fncom.2016.00129.

Lazarev, V.V., Simpson, D.M., Schubsky, B.M., DeAzevedo, L.C., 2001. Photic driving in the electro-encephalogram of children and adolescents: harmonic structure and relation to the resting state. Braz. J. Med. Biol. Res. 34, 1573–1584. https://doi.org/10.1590/S0100-879X2001001200010.

Lopes da Silva, F.H., Harding, G.F.A., 2011. Transition to seizure in photosensitive epilepsy. Epilepsy Res. 97, 278–282. https://doi.org/10.1016/j.eplepsyres.2011.10.022.

Lopes da Silva, F.H., Hoeks, A., Smits, H., Zetterberg, L.H., 1974. Model of brain rhythmic activity. Kybernetik 15, 27–37. https://doi.org/10.1007/BF00270757.

Lopes da Silva, F.H., van Rotterdam, A., Barts, P., van Heusden, E., Burr, W., 1976. Models of neuronal populations: the basic mechanisms of rhythmicity. Prog. Brain Res. 45, 281–308. https://doi.org/10.1016/S0079-6123(08)60995-4.

Lopes da Silva, F.H., Pijn, J.P., Velis, D., Nijssen, P.C., 1997. Alpha rhythms: noise, dynamics and models. Int. J. Psychophysiol. 26, 237–249. https://doi.org/10.1016/S0167-8760(97)00767-8.

Lopes da Silva, F., Blanes, W., Kalitzin, S.N., Parra, J., Suffczynski, P., Velis, D.N., 2003. Epilepsies as dynamical diseases of brain systems: basic models of the transition between normal and epileptic activity. Epilepsia 44 (Suppl. 1), 72–83.

Malow, A., Bowes, R.J., Ross, D., 2000. Relationship of temporal lobe seizures to sleep and arousal: a combined scalp-intracranial electrode study. Sleep 23, 231–234.

Marshall, L., Mölle, M., Fehm, H.L., Born, J., 1998. Scalp recorded direct current brain potentials during human sleep. Eur. J. Neurosci. 10, 1167–1178. https://doi.org/10.1046/j.1460-9568.1998.00131.x.

Marten, F., Rodrigues, S., Benjamin, O., Richardson, M.P., Terry, J.R., 2009a. Onset of polyspike complexes in a mean-field model of human electroencephalography and its application to absence epilepsy. Philos. Trans. R. Soc. A Math. Phys. Eng. Sci. 367, 1145–1161. https://doi.org/10.1098/rsta.2008.0255.

Marten, F., Rodrigues, S., Suffczynski, P., Richardson, M.P., Terry, J.R., 2009b. Derivation and analysis of an ordinary differential equation mean-field model for studying clinically recorded epilepsy dynamics. Phys. Rev. E - Stat. Nonlinear Soft Matter Phys. 79, 1–7. https://doi.org/10.1103/PhysRevE.79.021911.

Medvedeva, T.M., Sysoeva, M.V., van Luijtelaar, G., Sysoev, I.V., 2018. Modeling spike-wave discharges by a complex network of neuronal oscillators. Neural Network. 98, 271–282. https://doi.org/10.1016/j.neunet.2017.12.002.

Meeren, H.K.M., Pijn, J.P.M., Van Luijtelaar, E.L.J.M., Coenen, A.M.L., Lopes da Silva, F.H., 2002. Cortical focus drives widespread corticothalamic networks during spontaneous absence seizures in rats. J. Neurosci. 22, 1480–1495. https://doi.org/10.1557/JMR.1994.0401.

Meeren, H., van Luijtelaar, G., Lopes da Silva, F., Coenen, A., 2005. Evolving concepts on the pathophysiology of absence seizures: the cortical focus theory. Arch. Neurol. 62, 371–376. https://doi.org/10.1001/archneur.62.3.371.

Michels, L., Bucher, K., Brem, S., Halder, P., Lüchinger, R., Liechti, M., Martin, E., Jeanmonod, D., Kröll, J., Brandeis, D., 2011. Does greater low frequency EEG activity in normal immaturity and in children with epilepsy arise in the same neuronal network? Brain Topogr. 24, 78–89. https://doi.org/10.1007/s10548-010-0161-y.

Miranda de Sá, A.M.F.L., Infantosi, A.F.C., 2005. Evaluating the entrainment of the alpha rhythm during stroboscopic flash stimulation by means of coherence analysis. Med. Eng. Phys. 27, 167–173. https://doi.org/10.1016/j.medengphy.2004.09.011.

Moeller, F., LeVan, P., Muhle, H., Stephani, U., Dubeau, F., Siniatchkin, M., Gotman, J., 2010. Absence seizures: individual patterns revealed by EEG-fMRI. Epilepsia 51, 2000–10. https://doi.org/10.1111/j.1528-1167.2010.02698.x.

Mori, T., Kai, S., 2002a. Noise-induced entrainment and stochastic resonance in human brain waves. Phys. Rev. Lett. 88, 218101. https://doi.org/10.1103/PhysRevLett.88.218101.

Mori, T., Kai, S., 2002b. Stochastic resonance in alpha oscillators in the human brain. Int. J. Bifurc. Chaoshaos 12, 2631–2639. https://doi.org/10.1142/S0218127402006151.

Nagarajan, L., Kulkarni, A., Palumbo-Clark, L., Gregory, P.B., Walsh, P.J., Gubbay, S.S., Silberstein, J.M., Silberstein, E.P., Carty, E.L., Dimitroff, W.R., 2003. Photoparoxysmal responses in children: their characteristics and clinical correlates. Pediatr. Neurol. 29, 222–226. https://doi.org/10.1016/S0887-8994(03)00207-8.

Niedermeyer, Ernst, Lopes da Silva, F.H. (Eds.), 2005. Electroencephalography :Basic Principles, Clinical Applications, and Related Fields, fifth ed. Lippincott Williams & Wilkins.

Nunez, P.L., 2000. Toward a quantitative description of large-scale neocortical dynamic function and EEG. Behav. Brain Sci. 23, 371–398 discussion 399-437. https://doi.org/10.1017/S0140525X00003253.

Patel, V.M., Maulsby, R.L., 1987. How hyperventilation alters the electroencephalogram: a review of controversial viewpoints emphasizing neurophysiological mechanisms. J. Clin. Neurophysiol. 4, 101–120.

Petersén, I., Eeg-Olofsson, O., 1971. The development of the electroencephalogram in normal children from the age of 1 through 15 years. Non-paroxysmal activity. Neuropadiatrie 2, 247–304.

Polack, P.-O., Guillemain, I., Hu, E., Deransart, C., Depaulis, A., Charpier, S., 2007. Deep layer somatosensory cortical neurons initiate spike-and-wave discharges in a genetic model of absence seizures. J. Neurosci. 27, 6590–6599. https://doi.org/10.1523/JNEUROSCI.0753-07.2007.

Roberts, J.A., Robinson, P.A., 2008. Modeling absence seizure dynamics: implications for basic mechanisms and measurement of thalamocortical and corticothalamic latencies. J. Theor. Biol. 253, 189–201. https://doi.org/10.1016/j.jtbi.2008.03.005.

Roberts, J.A., Robinson, P.A., 2012. Quantitative theory of driven nonlinear brain dynamics. Neuroimage 62, 1947–55. https://doi.org/10.1016/j.neuroimage.2012.05.054.

Robinson, P.A., Rennie, C.J., Rowe, D.L., 2002. Dynamics of large-scale brain activity in normal arousal states and epileptic seizures. Phys. Rev. E 65, 041924. https://doi.org/10.1103/PhysRevE.65.041924.

Robinson, P.A., Rennie, C.J., Rowe, D.L., O'Connor, S.C., Wright, J.J., Gordon, E., Whitehouse, R.W., 2003. Neurophysical modeling of brain dynamics. Neuropsychopharmacology 28, S74–S79. https://doi.org/10.1038/sj.npp.1300143.

Rodrigues, S., Barton, D., Szalai, R., Benjamin, O., Richardson, M.P., Terry, J.R., 2009. Transitions to spike-wave oscillations and epileptic dynamics in a human cortico-thalamic mean-field model. J. Comput. Neurosci. 27, 507–526. https://doi.org/10.1007/s10827-009-0166-2.

Rosanova, M., Casali, A., Bellina, V., Resta, F., Mariotti, M., Massimini, M., 2009. Natural frequencies of human corticothalamic circuits. J. Neurosci. 29, 7679–7685. https://doi.org/10.1523/JNEUROSCI.0445-09.2009.

Ruff, D.A., Cohen, M.R., 2016. Attention increases spike count correlations between visual cortical areas. J. Neurosci. 36, 7523–7534. https://doi.org/10.1523/JNEUROSCI.0610-16.2016.

Sadleir, L.G., Scheffer, I.E., Smith, S., Carstensen, B., Carlin, J., Connolly, M.B., Farrell, K., 2008. Factors influencing clinical features of absence seizures. Epilepsia 49, 2100–2107. https://doi.org/10.1111/j.1528-1167.2008.01708.x.

Salchow, C., Strohmeier, D., Klee, S., Jannek, D., Schiecke, K., Witte, H., Nehorai, A., Haueisen, J., 2016. Rod driven frequency entrainment and resonance phenomena. Front. Hum. Neurosci. 10, 1–12. https://doi.org/10.3389/fnhum.2016.00413.

Salvati, K.A., Beenhakker, M.P., 2019. Out of thin air: hyperventilation-triggered seizures. Brain Res. 703, 41–52. https://doi.org/10.1016/j.brainres.2017.12.037.

Schwab, K., Ligges, C., Jungmann, T., Hilgenfeld, B., Haueisen, J., Witte, H., 2006. Alpha entrainment in human electroencephalogram and magnetoencephalogram recordings. Neuroreport 17, 1829–1833. https://doi.org/10.1097/01.wnr.0000246326.89308.ec.

Seneviratne, U., Cook, M., D'Souza, W., 2014. Focal abnormalities in idiopathic generalized epilepsy: a critical review of the literature. Epilepsia 55, 1157–1169. https://doi.org/10.1111/epi.12688.

Sohanian Haghighi, H., Markazi, A.H.D., 2017. A new description of epileptic seizures based on dynamic analysis of a thalamocortical model. Sci. Rep. 7, 13615. https://doi.org/10.1038/s41598-017-13126-4.

Spiegler, A., Knösche, T.R., Schwab, K., Haueisen, J., Atay, F.M., 2011. Modeling brain resonance phenomena using a neural mass model. PLoS Comput. Biol. 7, e1002298. https://doi.org/10.1371/journal.pcbi.1002298.

Stafstrom, C.E., Carmant, L., 2015. Seizures and epilepsy: an overview for neuroscientists. Cold Spring Harb. Perspect. Med. 5 a022426–a022426. https://doi.org/10.1101/cshperspect.a022426.

Stam, C.J., Pijn, J.P.M., Suffczynski, P., Lopes da Silva, F.H., 1999. Dynamics of the human alpha rhythm: evidence for non-linearity? Clin. Neurophysiol. 110, 1801–1813. https://doi.org/10.1016/S1388-2457(99)00099-1.

Steriade, M., 1974. Interneuronal epileptic discharges related to spike-and-wave cortical seizures in behaving monkeys. Electroencephalogr. Clin. Neurophysiol. 37, 247–263. https://doi.org/10.1016/0013-4694(74)90028-5.

Steriade, M., Yossif, G., 1974. Spike-and-wave afterdischarges in cortical somatosensory neurons of cat. Electroencephalogr. Clin. Neurophysiol. 37, 633–648. https://doi.org/10.1016/0013-4694(74)90076-5.

Suffczynski, P., Kalitzin, S., Pfurtscheller, G., Lopes da Silva, F.H., 2001. Computational model of thalamo-cortical networks: dynamical control of alpha rhythms in relation to focal attention. Int. J. Psychophysiol. 43, 25–40. https://doi.org/10.1016/S0167-8760(01)00177-5.

Suffczynski, P., Kalitzin, S., Lopes Da Silva, F.H., 2004. Dynamics of non-convulsive epileptic phenomena modeled by a bistable neuronal network. Neuroscience 126, 467–484. https://doi.org/10.1016/j.neuroscience.2004.03.014.

Taylor, P.N., Baier, G., 2011. A spatially extended model for macroscopic spike-wave discharges. J. Comput. Neurosci. 31, 679–684. https://doi.org/10.1007/s10827-011-0332-1.

Taylor, P.N., Baier, G., Cash, S.S., Dauwels, J., Slotine, J.-J., Wang, Y., 2013a. A model of stimulus induced epileptic spike-wave discharges. In: 2013 IEEE Symposium on Computational Intelligence, Cognitive Algorithms, Mind, and Brain (CCMB). IEEE, pp. 53–59. https://doi.org/10.1109/CCMB.2013.6609165.

Taylor, P.N., Goodfellow, M., Wang, Y., Baier, G., 2013b. Towards a large-scale model of patient-specific epileptic spike-wave discharges. Biol. Cybern. 107, 83–94. https://doi.org/10.1007/s00422-012-0534-2.

Taylor, P.N., Thomas, J., Sinha, N., Dauwels, J., Kaiser, M., Thesen, T., Ruths, J., 2015. Optimal control based seizure abatement using patient derived connectivity. Front. Neurosci. 9, 202. https://doi.org/10.3389/fnins.2015.00202.

Topalkara, K., Alarcón, G., Binnie, C.D., 1998. Effects of flash frequency and repetition of intermittent photic stimulation on photoparoxysmal responses. Seizure 7, 249–255. https://doi.org/10.1016/S1059-1311(98)80044-7.

Uhlrich, D.J., Manning, K.A., O'Laughlin, M.L., Lytton, W.W., 2005. Photic-induced sensitization: acquisition of an augmenting spike-wave response in the adult rat through repeated strobe exposure. J. Neurophysiol 94, 3925–3937. https://doi.org/10.1152/jn.00724.2005.

Veltz, R., Sejnowski, T.J., 2015. Periodic forcing of inhibition-stabilized networks: nonlinear resonances and phase-amplitude coupling. Neural Comput. 27, 2477–2509. https://doi.org/10.1162/NECO_a_00786.

Vyazovskiy, V.V., Olcese, U., Lazimy, Y.M., Faraguna, U., Esser, S.K., Williams, J.C., Cirelli, C., Tononi, G., 2009. Cortical firing and sleep homeostasis. Neuron 63, 865–878. https://doi.org/10.1016/j.neuron.2009.08.024.

Wagner, F.B., Truccolo, W., Wang, J., Nurmikko, A.V., 2015. Spatiotemporal dynamics of optogenetically induced and spontaneous seizure transitions in primary generalized epilepsy. J. Neurophysiol. 113, 2321–2341. https://doi.org/10.1152/jn.01040.2014.

Waltz, S., Christen, H.J., Doose, H., 1992. The different patterns of the photoparoxysmal response - a genetic study. Electroencephalogr. Clin. Neurophysiol. 83, 138–145. https://doi.org/10.1016/0013-4694(92)90027-F.

Wang, Y., Goodfellow, M., Taylor, P.N., Baier, G., 2012. Phase space approach for modeling of epileptic dynamics. Phys. Rev. E. Stat. Nonlin. Soft Matter Phys. 85, 061918. https://doi.org/10.1103/PhysRevE.85.061918.

Wendling, F., Benquet, P., Bartolomei, F., Jirsa, V., 2016. Computational models of epileptiform activity. J. Neurosci. Methods 260, 233–251. https://doi.org/10.1016/j.jneumeth.2015.03.027.

Wiesenfeld, K., Moss, F., 1995. Stochastic resonance and the benefits of noise: from ice ages to crayfish and SQUIDs. Nature 373, 33–36. https://doi.org/10.1038/373033a0.

Yang, D.P., Robinson, P.A., 2017. Critical dynamics of Hopf bifurcations in the corticothalamic system: transitions from normal arousal states to epileptic seizures. Phys. Rev. E 95. https://doi.org/10.1103/PhysRevE.95.042410.

Zaehle, T., Lenz, D., Ohl, F.W., Herrmann, C.S., 2010. Resonance phenomena in the human auditory cortex: individual resonance frequencies of the cerebral cortex determine electrophysiological responses. Exp. Brain Res. 203, 629–635. https://doi.org/10.1007/s00221-010-2265-8.

Zetterberg, L.H., Kristiansson, L., Mossberg, K., 1978. Performance of a model for a local neuron population. Biol. Cybern. 31, 15–26. https://doi.org/10.1007/BF00204593.

Zhao, X., Robinson, P.A., 2017. Neural field model of seizure-like activity in isolated cortex. J. Comput. Neurosci. 42, 307–321. https://doi.org/10.1007/s10827-017-0642-z.